COBEM UBERLÂNDIA 2019

ABCM Associação Brasileira de Engenharia e Ciências Mecânicas

25th ABCM International Congress of Mechanical Engineering
October 20-25, 2019, Uberlândia, MG, Brazil

COB-2019-0129
EFFECTS OF YAW MISALIGNMENT ON WIND TURBINE POWER PRODUCTION

Bruno Mitsuo Mazetto
Thiago Gamboa Ritto
Universidade Federal do Rio de Janeiro
bmazetto@gmail.com
tritto@mecanica.ufrj.br

Abstract. *The effects of yaw misalignment on the power curve of a 5-MW reference offshore wind turbine and on the expected annual energy production for wind conditions of offshore sites in UK and Brazil were studied. The goal was to determine a reduction factor to be used as input for new wind farm projects. To achieve the results, Monte Carlo simulations using the open source FAST (Fatigue, Aerodynamics, Structures and Turbulence) code for wind turbine simulation were performed and a stochastic approach was considered for the wind speed and yaw misalignment. Considering the effects of yaw misalignment, an effective power curve for the 5-MW reference offshore wind turbine was obtained. Moreover, the yaw misalignment generated an annual energy production decreasing factor between 3% and 5%.*

Keywords: *Yaw misalignment, Wind energy, Wind turbine, Stochastic model, Monte Carlo simulation*

1. INTRODUCTION

Over the last decades, wind power has become one of the most attractive renewable energy sources and a promising competitor against fossil fuel-based energy. Onshore and, most recently, offshore wind farms have spread out all over the world due to decreasing costs and government incentives. According to the Global Wind Energy Council - GWEC (2016), by the end of 2018, there were over 550 GW of installed wind power capacity, an amount 20 times greater than that from the beginning of the century. Moreover, the global market has been growing about 50 GW/year.

Along with the market itself, the technology behind it has experienced fast improvement. For instance, in 1985 a typical wind turbine would deliver a rated power of only 0.05 MW with a 15-meter rotor (International Renewable Energy Agency - IRENA, 2019). Nowadays, for offshore applications, there are 10 MW commercially available turbines with rotor diameter of 164 meters (MHI Vestas, 2018). And for the near future, GE Renewable Energy has already announced the Heliade-X 12 MW, the biggest offshore wind turbine, with a 220-meter rotor (General Electric - GE, 2018).

Despite the technology evolution and the increase in size and rated power of horizontal axis wind turbines, a basic strategy for getting the most out of the wind resource is to align the rotor axis with the wind direction, what is called yaw alignment (Kragh and Hansen, 2015). To do so, MW-class wind turbines are supplied with a yaw drive mechanism and a control system that turns the nacelle according to wind direction measurements (Choi *et al.*, 2018). A schematic view of the yaw system can be seen in Fig. 1.

Although there is a dedicated control system to cope with yaw misalignment, it is still a reality for wind turbines. Hojstrup (2014) presented the results from approximately 100 measurements of yaw error using a spinner anemometer and concluded that about half of the turbines lost at least 1% of annual energy production (AEP) as a result of these errors. Fleming *et al.* (2014) indicated that a 7.5° of yaw misalignment was responsible for a 2.4% loss of AEP. Steinmetz (2016) points out that correcting yaw misalignment could lead, in average, to a 2% gain in AEP. Moreover, Choi *et al.* (2018), Steinmetz (2016) and Hojstrup (2014) mentioned increased fatigue loads on the blades, drive train and hub, which could cause premature failure of components.

As classified by Choi *et al.* (2018), yaw misalignment could be divided into two categories, static and dynamic. The first one represents the mean error during an observation period and remains constant throughout the operation of the wind turbine. It is mainly caused by improper installation or poor calibration of the wind vane sensor, as well as, loosening of sensor mountings thanks to vibration. In opposition, the dynamic error represents the instantaneous difference between the total and the static misalignment. Its fundamental causes are wind flow distortion by blade's activities, terrain complexity or wakes of neighboring wind turbines, along with yaw control system tolerance. Some level of error is tolerated by the yaw controller for safety and efficiency reasons.

In this paper, the aim is to assess the effects of yaw misalignment on the power curve of a 5-MW reference offshore

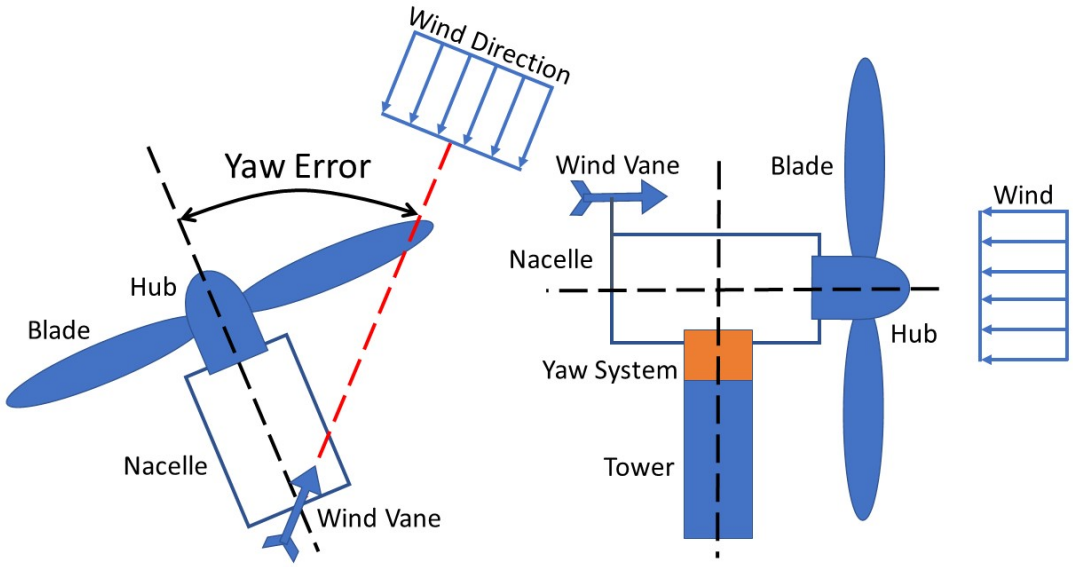

Figure 1: Schematic view of yaw system and yaw error.

wind turbine and expected annual energy production for two different wind conditions, one from an offshore wind farm in the United Kingdom and another from an offshore site in the Northeast coast of Brazil. The goal is to determine a reduction factor to be used as input for new wind farm projects. Next, the employed methodology will be presented.

2. METHODOLOGY

To understand how the yaw error affects the wind turbine power production, the following steps were taken into consideration: (1) Definition of the wind turbine; (2) Definition of the stochastic model for the uncertain parameters; (3) Running Monte Carlo simulations to get statistics on power production. In the next sub-items, each step will be described.

2.1 Wind turbine model

For this study, the NREL offshore 5-MW baseline wind turbine from Jonkman *et al.* (2009) was considered. The model is based on public information from Multibrid M5000 and REpower 5M prototype wind turbines and was developed to serve as a standardized input data in studies aimed at assessing offshore wind technology suitable in shallow and deep waters off the U. S. offshore continental shelf.

The model represents a 5-MW, three-bladed, upwind horizontal axis wind turbine. It has a rotor diameter of 126 m and its hub is at a height of 90 m above the base of the wind turbine's tower. Power generation starts when wind speed reaches 3 m/s, increases until it gets to 11.4 m/s, when rated power is achieved, and is kept constant from 11.4 m/s to 25 m/s. For speeds higher than 25 m/s, power production is interrupted to avoid system overload.

2.2 Stochastic model

For the simulations, the inputs assumed to be random variables were the wind speed and the yaw misalignment.

2.2.1 Wind speed

The probability distribution function for the wind speed were obtained by fitting a Weibull distribution to data retrieved from the ERA5 reanalysis dataset, through the use of the software WindPRO v3.1. Wind speed at hub height from the year 2000 to 2018, which were all the available public data, was considered for the curve fitting for two locations: London Array Offshore Wind Farm center location, available in 4C Offshore (2019b), and EOL Planta Piloto de Geração Offshore, available in 4C Offshore (2019a).

The Weibull distribution function is shown in Eq. (1), where k and c are the shape and the scale parameters, respectively.

$$f_V(v) = \left(\frac{k}{c}\right)\left(\frac{v}{c}\right)^{k-1} exp\left[\left(\frac{v}{c}\right)^{k}\right] \tag{1}$$

London Array has a installed capacity of 630 MW. It occupies an area of 100 km^2 on the coast of the United Kingdom, as stated by London Array (2019). The wind speed at the center of the wind farm is represented by a Weibull distribution with $k = 2.32$ and $c = 10.1$, which leads to a mean speed of 9.0 m/s. On the other hand, EOL Planta Piloto de Geração Offshore is a R&D Project being developed by Petrobras. According to 4C Offshore (2019a), a 5-MW turbine is being considered to be installed on the Northeast coast of Brazil. The wind speed at the wind turbine location is represented by a Weibull distribution with $k = 4.74$ and $c = 9.7$, which leads to a mean speed of 8.9 m/s. The probability density functions for both locations are plotted together and displayed in Fig. 2.

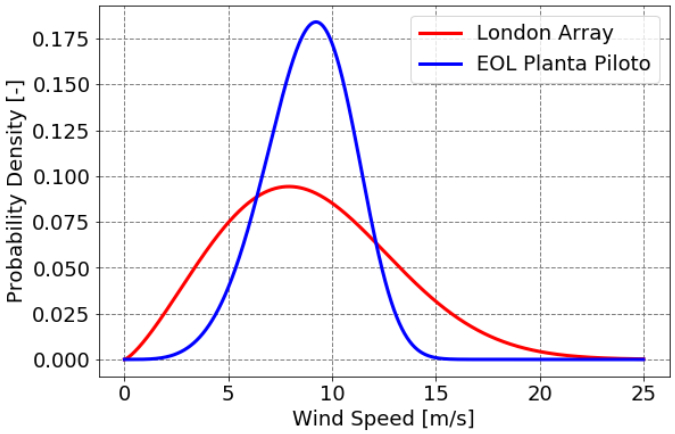

Figure 2: Probability density function for the wind speeds.

2.2.2 Yaw misalignment

As considered by Choi *et al.* (2018), the total yaw misalignment is composed of a static element, which is the mean value of the observations, and by a dynamic element. Considering the data presented by Hojstrup (2014), it was assumed that the mean yaw misalignment would behave as a Gaussian distribution with zero mean and 8° of standard deviation, as displayed in Fig. 6.

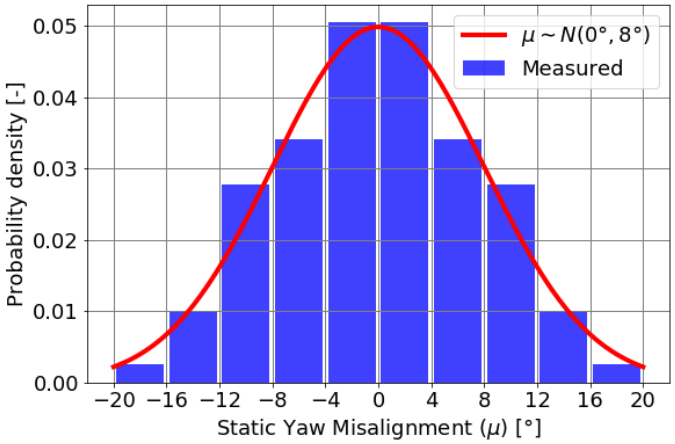

Figure 3: PDF considered for static yaw misalignment, based on Hojstrup (2014).

Regarding the dynamic element, Schlipf *et al.* (2011) and Song *et al.* (2018) indicated that the variation would have a Gaussian distribution with zero mean. From Song *et al.* (2018), it was obtained a standard deviation of 10° for the Gaussian distribution assumed for this study, as seen in Fig. 4.

To get the total yaw misalignment for a single simulation, one should get firstly the mean value of the distribution and afterwards, obtain the result of static and dynamic components altogether. The procedure is shown in Fig. 5.

An important observation is that, in this study, it was assumed that the yaw misalignment and wind speed are independent random variables. According to Kragh and Hansen (2015) and Hojstrup (2014), the total yaw error tends to become smaller as wind gets faster. However, they have also noted that once the wind speed is above the rated value, yaw misalignment effects on power production are reduced. Since the goal of this study is to assess the performance reduction due to yaw misalignment as an input parameter for economic evaluation of new projects, the possible overestimation of power loss is a conservative result.

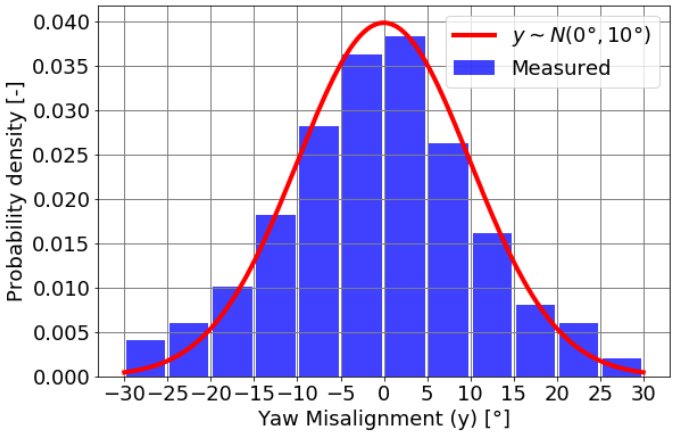

Figure 4: PDF for total yaw misalignment with no static component, based on Song *et al.* (2018).

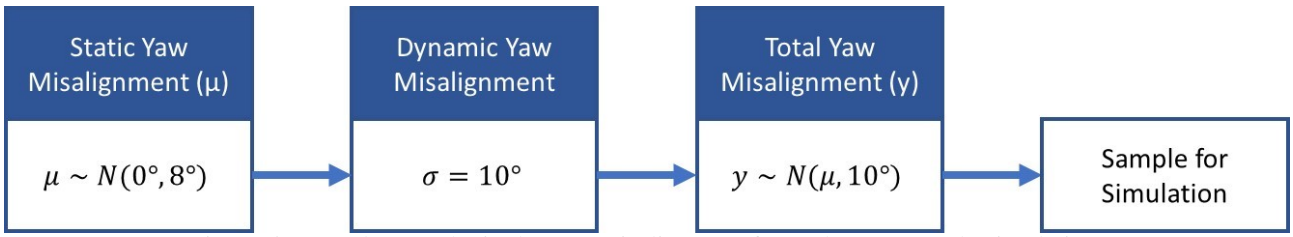

Figure 5: Procedure to obtain the yaw misalignment for each Monte Carlo simulation.

2.3 Monte Carlo simulations

The simulation tool used to obtain the power produced for each pair of wind speed and total yaw misalignment was the 8^{th} version of NREL FAST (Fatigue, Aerodynamics, Structures and Turbulence) Code, an open source framework composed of different modules that together provide a coupled aero-hydro-servo-elastic solution for wind turbine simulation (Jonkman and Jonkman, 2016).

Jonkman (2013) showed that the structural-dynamic model for horizontal-axis wind turbines employed in FAST possess 24 degrees of freedom, considering the possible motions of blades, drivetrain, nacelle, tower and platform. The formulation is based on a combination of multi-body and modal dynamics, the former being used for the platform, nacelle and drivetrain, and the latter, for the blades and tower. Kane's method is used to obtain equations of motion, with the form shown in Eq. (2).

$$\mathbf{M}\left(\mathbf{q},\mathbf{u},t\right)\dot{\mathbf{q}}+\mathbf{f}\left(\mathbf{q},\dot{\mathbf{q}},\mathbf{u},\dot{\mathbf{u}},t\right)=\mathbf{0} \tag{2}$$

The first and second terms in Eq. (2) are known as the sum of generalized inertia forces and active forces, respectively. Both terms are dependent of time t and generalized coordinates q and speeds u. External forces acting on the system are aerodynamic and hydrodynamic loads and controller commands (Jonkman, 2013).

The following premises were taken into account for each simulation:

1. The wind turbine is installed on a fixed-bottom substructure;
2. Wake effects due to other wind turbines are not considered;
3. Waves and currents effects are not considered for the simulations;
4. Steady wind conditions;
5. Yaw misalignment is kept constant;
6. Two independent control strategies are adopted: a generator-torque controller, that maximizes power capture below the rated operation point, and a full-span rotor-collective blade-pitch controller, which regulates the generator speed above the rated operation point (Jonkman *et al.*, 2009).

Regarding convergence of simulations, the mean square convergence was adopted considering power production as the output parameter. It was observed that the use of 500 simulations was enough to guarantee the convergence of all Monte Carlo simulations.

2.4 Annual energy production (AEP)

In order to calculate AEP, the first step is to obtain the capacity factor (C_F). As presented by Letcher (2017), C_F is given by Eq. (3), where E_{actual} stands for the actual energy generated over a given period of time and E_{ideal} is the energy that would be generated if the wind turbine were operated at rated power over the same given period of time.

$$C_F = \frac{E_{actual}}{E_{ideal}} = \frac{P_{average} \cdot Time}{P_{rated} \cdot Time} = \frac{P_{average}}{P_{rated}} \tag{3}$$

Once C_F is known, Letcher (2017) indicates that the annual energy production can be calculated using Eq. (4), where T_{year} is the amount of hours in one year.

$$AEP = P_{rated} \cdot C_F \cdot T_{year} \tag{4}$$

3. RESULTS

3.1 Effective power curve

To get the effective power curve, after accounting for the yaw misalignment, Monte Carlo simulations were performed for a few fixed wind speeds, marked as black circles in Fig. 6a. The red area represents a 98% stochastic envelope and the dashed black line is the mean value of power production. The connection between each speed is made through linear interpolation.

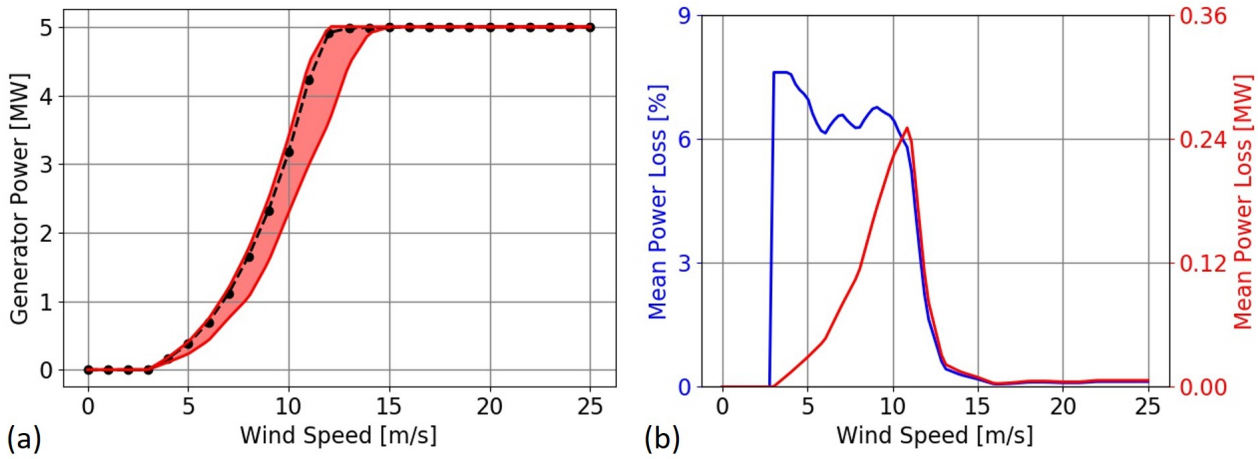

Figure 6: (a) Effective power curve of the NREL 5-MW wind turbine; (b) Mean power loss.

Figure 6a shows that the range of power production increases as the wind speed rises and is the largest near the rated wind speed. However, the mean value of power for each wind speed is always close to left boundary of the stochastic envelope, which is the nominal power curve, as presented by Jonkman *et al.* (2009). Figure 6b indicates the percentual and absolute power loss between the maximum and mean power. It is possible to see that the percentual losses have a decreasing tendency and are between 6% and 8% of the actual power curve. In terms of absolute losses, they increase from cut-in to rated wind speed, where the losses reach 0.24 MW.

3.2 Annual energy production

For the sake of comparison, Monte Carlo simulations were executed for no yaw misalignment conditions and also for the yaw misalignment presented in subsection 2.2. Both wind scenarios were considered. The results are given in Tab. 1.

Table 1: Capacity factor and annual energy production for London Array and EOL Planta Piloto wind conditions.

	London Array		EOL Planta Piloto	
Yaw Misalignment	No	Yes	No	Yes
Average Power ($P_{average}$)	2.54 MW	2.42 MW	2.49 MW	2.42 MW
Capacity Factor (C_F)	50.9 %	48.5 %	50.0 %	48.4 %
Annual Energy Production (AEP)	22.3 GWh	21.2 GWh	21.9 GWh	21.2 GWh
Decrease in (AEP)	-	4.8 %	-	3.1 %

Table 1 shows that, for simulations considering no yaw error, the average power production at steady state is 2.54 MW for London Array and 2.50 MW for EOL Planta Piloto. When the yaw misalignment is taken into account, average power production decreases to 2.42 MW for both locations. For London Array location, the yaw error causes almost 5% of energy production loss. For EOL Planta Piloto location, it reduces the energy production in about 3%. It leads to the conclusion that the intensity of the yaw misalignment effect on annual energy production depends on the wind speed probability density function of the location considered.

4. CONCLUSIONS

In this study, the effects of yaw misalignment on the power curve of a 5-MW reference offshore wind turbine and on the expected annual energy production for wind conditions of offshore sites in UK and Brazil were studied. The goal was to determine a reduction factor to be used as input for new wind farm projects. To achieve the results, Monte Carlo simulations using the open source FAST code for wind turbine simulation were performed and a stochastic approach was considered for the wind speed and yaw misalignment.

Considering the effects of yaw misalignment, an effective power curve for the 5-MW reference offshore wind turbine was obtained. This curve can be used for power production calculations for any wind speed conditions. Moreover, for the wind speed probability density functions studied, the yaw misalignment generated an AEP decreasing factor between 3% and 5%. These values could be used during the economic evaluation of wind projects, providing a more accurate view of their feasibility.

5. ACKNOWLEDGEMENTS

This paper was developed as part of Petrobras "Offshore Wind Pilot Plant" project (PD-0553-0045 / 2016) within the framework of the Electric System R&D, regulated by ANEEL.

6. REFERENCES

4C Offshore, 2019a. "Eol planta piloto de geração offshore – project details". <https://www.4coffshore.com/windfarms/paracuru-campo-eolico-brazil-br26.html>.

4C Offshore, 2019b. "London array offshore wind farm – project details". <https://www.4coffshore.com/windfarms/london-array-phase-1-united-kingdom-uk14.html>.

Choi, D., Shin, W., Ko, K. and Rhee, W., 2018. "Static and dynamic yaw misalignments of wind turbines and machine learning based correction methods using lidar data". *IEEE Transactions on Sustainable Energy*, Vol. PP, pp. 1–1.

Fleming, P., Scholbrock, A. and Wright, A., 2014. "Field test results of using a nacelle-mounted lidar for improving wind energy capture by reducing yaw misalignment (presentation)". In *Nordic Wind Power Conference 2014*. Sweden, Scotland.

General Electric - GE, 2018. "Ge announces haliade-x, the world's most powerful offshore wind turbine". <https://www.genewsroom.com/press-releases/ge-announces-haliade-x-worlds-most-powerful-offshore-wind-turbine-284260>.

Global Wind Energy Council - GWEC, 2016. "Global wind report 2018". April 2019. <https://gwec.net/global-wind-report-2018/>.

Hojstrup, J., 2014. "Increased energy production by optimization of yaw control". *VGB PowerTech*, Vol. 6, pp. 62–66.

International Renewable Energy Agency - IRENA, 2019. "Wind power - technology brief". March 2016. <https://www.irena.org/publications/2016/Mar/Wind-Power>.

Jonkman, B. and Jonkman, J., 2016. *FAST v8.16.00a-bjj*. National Renewable Energy Laboratory, Golden.

Jonkman, J., 2013. "Overview of the elastodyn structural-dynamics module". In *EWEA Offshore 2013*. Frankfurt, Germany.

Jonkman, J., Butterfield, S., Musial, W. and Scott, G., 2009. *Technical Report No. NREL/TP-500-38060: Definition of a 5-MW reference wind turbine for offshore system development*. National Renewable Energy Laboratory, Golden.

Kragh, K.A. and Hansen, M.H., 2015. "Potential of power gain with improved yaw alignment". *Wind Energy*, Vol. 18, pp. 979–989.

Letcher, T.M., 2017. *Wind Energy Engineering – A Handbook for Onshore and Offshore Wind Turbines*. Academic Press, Cambridge.

London Array, 2019. "London array brochure". January 2019. <http://www.londonarray.com/wp-content/uploads/London-Array-Brochure.pdf>.

MHI Vestas, 2018. "Mhi vestas launches the first 10 mw wind turbine in history". <http://www.mhivestasoffshore.com/mhi-vestas-launches-the-first-10-mw-wind-turbine-in-history/>.

Schlipf, D., Rettenmeier, A., Martin, K., Kapp, S., Anger, J., Bischoff, O., Hofs, M., Hofsäß, M. and Kühn, M., 2011. "Prospects of optimization of energy production by lidar assisted control of wind turbines". In *EWEA 2011 Conference*

Proceedings. Brussels, Belgium.

Song, D., Yang, J., Fan, X., Liu, Y., Liu, A., Chen, G. and Joo, Y.H., 2018. "Maximum power extraction for wind turbines through a novel yaw control solution using predicted wind directions". *Energy Conversion and Management*, Vol. 157, pp. 587–599.

Steinmetz, G., 2016. "Wind analysis in operation phases: identifying and unlocking optimization capacities". In *Conférence sur l'exploitation des parcs éoliens 2016*. Paris, France.

7. RESPONSIBILITY NOTICE

The authors are the only responsible for the printed material included in this paper.